*Aust. J. Phys.*, 1986, **39**, 203–16

# An Analytic Distorted Wave Approximation for Electropion and Photopion Production on $^{12}C$ near Threshold

*F. Di Marzio and K. Amos*

School of Physics, University of Melbourne,
Parkville, Vic. 3052.

*Abstract*

An analytic distorted wave approximation (ADWA) that can be used to analyse photopion and electropion production cross sections is developed. An application is made to analyse data from $^{12}C$ near threshold once the approximation scheme is established as a realistic replacement for the more usual, distorted wavefunctions given by the optical model for low energy pion scattering. The pion production data analyses made using a generalized Helm model for the transition densities clearly demonstrates the significant role of distortion effects and that the ADWA is a good and simple representation of these effects. Repeating the analyses using microscopic models of nuclear structure indicates inadequacies in those structure specifications.

## 1. Introduction

The past few years have witnessed considerable experimental and theoretical activity in the field of charged pion photoproduction from nuclei and, in particular, from $^{12}C$. With the attainment of increased beam intensities and the development of high resolution spectrometers, interest will not only continue but expand in the future, allowing even more elaborate theoretical analyses to be pursued.

Recently quite complete experimental studies of photopion production from $^{12}C$ have been made by Shoda *et al.* (1980) and by Schmitt *et al.* (1983). Here we focus our attention on these experimental data and compare our predictions with other theoretical results. In fact, from a theoretical viewpoint, considerable effort has already been directed towards examining the importance of final state interactions and the choice of nuclear wavefunctions and interaction Hamiltonian (Nagl and Überall 1976; Epstein *et al.* 1978; Furui 1978; Singham *et al.* 1979; Haxton 1980; Singham and Tabakin 1981).

Previous analyses using a generalized Helm model prescription (Überall 1971; Cannata *et al.* 1974) produced reasonable fits to the data. However, even though the Helm model does not suffer from uncertainties in the nuclear wavefunctions and is attractively simple, it possesses the less attractive attribute of replacing the pion continuum wavefunction by a plane wave. In this paper we present an analytical means of approximating distortion and thus retaining computational convenience within the Helm model picture. Furthermore, once the relevant distortion parameters have been ascertained, various microscopic nuclear structure models may be tested using an appropriate transition density.

0004-9506/86/020203$02.00

The ADWA version of real and virtual photopion production cross sections near threshold is developed in Sections 2 and 3, and the utility and parameter values of the ADWA functions are discussed and specified from analyses of low energy pion elastic scattering data. An application to pion production from $^{12}C$ is made and the results are reported in Section 4.

## 2. Theory

Of the many studies of photoproduction of charged pions from nuclei, the more recent have included fully distorted wavefunctions for the emergent pions and all terms in the interaction Hamiltonian derivable from the complete transition operator relevant to the elementary process of pion photoproduction from a nucleon. In so doing, the computational effort is increased and a direct simple interpretation in terms of nuclear structure properties is made obscure in comparison with plane wave approximation studies.

For photon energies near threshold, just one term in the interaction Hamiltonian is of importance, namely

$$H_{\rm int} = -{\rm i}(2/E_\pi\, k_\gamma)^{\frac{1}{2}}(2\pi ef/m_\pi)\sum_{j=1}^{A}\boldsymbol{\sigma}_j.\boldsymbol{\xi}^\lambda\,\delta(r-r_j)\tau_j^\pm, \tag{1}$$

from which one obtains differential cross sections for photopion production (in $\mu{\rm b\,sr^{-1}}$) via

$${\rm d}\sigma/{\rm d}\Omega = 2\times10^4\, k_\gamma\, e^2f^2/\{p_\pi\, m_\pi^2(2J_{\rm i}+1)\}\sum_{M_{\rm i}M_{\rm f}}\sum_{\lambda}|\boldsymbol{\xi}^\lambda.\mathscr{M}|^2, \tag{2}$$

with the nuclear matrix elements

$$\mathscr{M} = \langle J_{\rm f}\,M_{\rm f}|\phi^*_{p_\pi}(r)\sum_{j=1}^{A}\boldsymbol{\sigma}_j\tau_j^\pm\,\exp({\rm i}\boldsymbol{k}_\gamma.\boldsymbol{r}_j)|\,J_{\rm i}\,M_{\rm i}\rangle. \tag{3}$$

As usual, $m_\pi$ and $E_\pi$ are the pion rest mass and total energy, $p_\pi$ and $k_\gamma$ are the pion and photon momenta, and $\xi$ is the photon polarization vector. The electromagnetic and pion–nucleon coupling constants $e^2$ and $f^2$ are $4\pi\alpha$ (the fine structure constant) and $0{\cdot}08\times(4\pi)$ respectively.

The photon polarization index sum yields

$$\sum_\lambda|\boldsymbol{\xi}^\lambda.\mathscr{M}|^2 = |\mathscr{M}|^2 = |\,\hat{\boldsymbol{k}}_\gamma.\mathscr{M}|^2, \tag{4}$$

where $\hat{\boldsymbol{k}}_\gamma$ is the unit vector in the photon direction.

The differential cross section for electropion production is then determined from the $(\gamma,\pi)$ results via (Shoda *et al.* 1980)

$$\left(\frac{{\rm d}\sigma(T_\pi)}{{\rm d}\Omega\,{\rm d}T_\pi}\right)_{{\rm e}\to\pi} = \sum_{E_{\rm f}}\left(\frac{{\rm d}\sigma(k_\gamma,E_{\rm f})}{{\rm d}\Omega}\right)_{\gamma\to\pi}N_{h\nu}(k_\gamma,T_{\rm e}), \tag{5}$$

where $T_{\rm e}$ and $T_\pi$ are the kinetic energies of the incident electron and emergent pion, $E_{\rm f}$ is the energy of the state in the residual nucleus and $N_{h\nu}(k_\gamma,T_{\rm e})$ is the virtual photon spectrum which can be evaluated using the Dalitz–Yennie (1957) formula.

In addition, as the electropion energy distribution is both angle and $E_f$ dependent, the allowed pion kinetic energies are found from

$$T_\pi = k_\pi^2/2m_\pi, \tag{6}$$

with

$$k_\pi = \left(\frac{1}{m_\pi}+\frac{1}{M}\right)^{-1}\left[\frac{k_\gamma}{M}\cos\theta+\left\{\left(\frac{k_\gamma}{M}\cos\theta\right)^2 +2\left(k_\gamma - m_\pi - \omega\frac{k_\gamma^2}{2M}\right)\left(\frac{1}{m_\pi}+\frac{1}{M}\right)\right\}^{\frac{1}{2}}\right]. \tag{7}$$

Here $M$ is the nuclear mass and $\omega$ is the energy difference between the ground state of the original nucleus and the final nuclear state. In this way only a specific range of pion energies is permitted for any particular value of $E_f$.

Near threshold therefore, the simplified interaction Hamiltonian yields cross-section formulae for both photopion and electropion production from nuclei that involve nuclear structure properties in a simple and straightforward manner (via the matrix elements $\mathscr{M}$), and which can be expressed in terms of the transition densities $\rho_{LL'}(r)$. Such densities can be chosen either as a convenient functional form (the Helm model) with parameter values obtained from other empirical data or from an appropriate nuclear structure calculation.

The pion wavefunction $\phi_{p_\pi}(r)$ contained in the matrix elements is best represented by the distorted wavefunction as determined from optical model analyses of the elastic scattering of pions at the relevant kinetic energies. If this distortion can be ignored, the resultant plane wave matrix elements are easily evaluated and the cross sections are proportional to Bessel transforms of the transition densities.

For pions with low kinetic energies (up to 40 MeV), the distortion is weak; the nucleus is relatively transparent and not strongly refractive. Thus, in analyses of photopion and electropion production near threshold, the usual distorted wavefunctions can be replaced using the analytic distorted wave approximation, for which

$$\phi^*_{p_\pi}(r) = N\exp\{-\mathrm{i}(\alpha+\mathrm{i}\beta)\boldsymbol{p}_\pi\cdot\boldsymbol{r}\}, \tag{8}$$

in which it is customary to use

$$N = \exp(-\beta p_\pi r_0 A^{1/3}) \tag{9}$$

to normalize the functions to unit magnitude at the nuclear surface. The parameter values $(\alpha, \beta)$ may be chosen by using the known optical model potential and the integral equation form for the elastic pion scattering amplitude to match the distorted wave calculations that best fit the measured data. Such a prescription has been used extensively and successfully (Di Marzio and Amos 1983, 1985*a*, 1985*b*) to determine ADWA parameters for intermediate energy protons, pions and kaons and, more recently (Amos and Di Marzio 1985), for antiprotons; it is used here to treat low energy pions (details are given in the next section).

Within this framework, the matrix elements of equation (3) may then be expressed as

$$\mathscr{M} = \langle J_f M_f|\sum_{l=1}^{A}\boldsymbol{\sigma}_l\tau_l^{\pm}\exp(\mathrm{i}\boldsymbol{Q}\cdot\boldsymbol{r}_l)|J_i M_i\rangle, \tag{10}$$

where $\boldsymbol{Q}$ is the complex momentum transfer given by

$$\boldsymbol{Q} = (\boldsymbol{k}_\gamma - \alpha \boldsymbol{p}_\pi) - \mathrm{i}\beta \boldsymbol{p}_\pi \tag{11}$$

$$= \boldsymbol{T} - \mathrm{i}\beta \boldsymbol{p}_\pi \tag{12}$$

and

$$T = (k_\gamma^2 - 2\alpha k_\gamma p_\pi \cos\theta + \alpha^2 p_\pi^2)^{\frac{1}{2}}. \tag{13}$$

The absorption of low energy pions by nuclei is weak ($\beta \sim 0$), as is deduced from the analyses we have made of the elastic scattering of 20 to 40 MeV pions and which is discussed subsequently, and as is expected since the Helm model ($\beta = 0$) predictions of the photoproduction cross sections are in good agreement with the data.

We may thus use the approximation $\boldsymbol{Q} = \boldsymbol{T}$ in our evaluations, which is then a simple modification of the plane wave theory by which the matrix elements of equation (10) may be expressed as (Überall 1971)

$$\mathscr{M} = \mp 4\pi \{2/(2J_\mathrm{f}+1)\}^{\frac{1}{2}} \sum_{LL'M} \langle J_\mathrm{i}\, LM_\mathrm{i}\, M | J_\mathrm{f}\, M_\mathrm{f}\rangle\, I_{LL'}(q)\, Y_{LL'}^{M*}(\hat{\boldsymbol{q}}), \tag{14}$$

where

$$\boldsymbol{q} = \boldsymbol{k}_\gamma - \boldsymbol{p}_\pi \tag{15}$$

is the usual momentum transfer and

$$I_{LL'}(q) = \mathrm{i}^{L'} \int r^2 \mathrm{j}_{L'}(qr)\, \rho^{\mathrm{if}}_{LL'}(r)\, \mathrm{d}r \tag{16}$$

is the transition form factor. The sign in equation (14) is determined from the raising (lowering) isospin operators.

In the generalized Helm model the transition densities $\rho^{\mathrm{if}}_{LL'}(r)$ are assumed to be peaked at a transition radius $\bar{R}$ in the form of a $\delta$ function, which is smeared out by a convolution with a gaussian $f_{\bar{g}}(q)$, i.e.

$$\rho^{\mathrm{if}}_{LL'}(r) = (2J_\mathrm{i}+1)^{\frac{1}{2}} \bar{\gamma}_{LL'}\, r^{-2} \delta(r - \bar{R})\, f_{\bar{g}}(q)\, \mathrm{i}^{-L'}, \tag{17}$$

with

$$f_{\bar{g}}(q) = \exp(-\tfrac{1}{2}\bar{g}^2 q^2). \tag{18}$$

The parameters $\bar{g}$, $\bar{R}$ and $\bar{\gamma}_{LL'}$ may be found by fitting the appropriate electron scattering data, as has been done in this case (Cannata *et al.* 1974). The values are listed in Table 1 for completeness.

Hence, the relevant matrix elements may be evaluated and, in the case of our ADWA version of the generalized Helm model, they are for electric multipole transitions

$$\sum_{M_\mathrm{i} M_\mathrm{f}} |\mathscr{M}|^2_{\mathrm{E}L} = 8\pi I^*_{LL}(T)\, I_{LL}(T), \tag{19}$$

$$\sum_{M_\mathrm{i} M_\mathrm{f}} |\hat{\boldsymbol{k}}_\gamma \cdot \mathscr{M}|^2_{\mathrm{E}L} = 8\pi I^*_{LL}(T)\, I_{LL}(T) \Bigg( \tfrac{1}{3} + (-)^L (\tfrac{3}{2})^{\frac{1}{2}} \langle LL00|20\rangle \times (2L+1) \begin{Bmatrix} L & L & 2 \\ 1 & 1 & L \end{Bmatrix} \{(\hat{\boldsymbol{k}}_\gamma \cdot \hat{\boldsymbol{T}})^2 - \tfrac{1}{3}\} \Bigg), \tag{20}$$

**Table 1. Helm model parameters used in analyses of photopion data (with $\bar{g} = 0{\cdot}77$ fm)**

| Excitation energy[A] (MeV) | $J^\pi$ | $\bar{R}$ (fm) | $\bar{\gamma}_{LL}$ | $\bar{\gamma}_{LL-1}$ | $\bar{\gamma}_{LL+1}$ |
|---|---|---|---|---|---|
| 13·37 | $1^+$ | 2·24 | | 0·97 | 0 |
| 14·32 | $2^+$ | 2·60 | 1·290 | | |
| 15·04 | $2^-$ | 2·82 | | 0·65 | −2·01 |
| 15·99 | $1^-$ | 1·70 | 0·247 | | |
| 16·09 | $1^-$ | 3·47 | 0·812 | | |
| 17·13 | $2^+$ | 2·67 | 0·019 | | |
| 17·70 | $1^-$ | 2·08 | 0·338 | | |
| 17·90 | $2^-$ | 2·97 | | 1·47 | −0·99 |
| 18·40 | $4^-$ | 2·82 | | 2·68 | 2·59 |
| 19·00 | $2^+$ | 2·50 | 0·421 | | |
| 19·10 | $3^+$ | 2·40 | | 0·72 | 2·22 |
| 20·00 | $3^-$ | 2·82 | 0·700 | | |
| 21·10 | $1^-$ | 2·60 | 0·829 | | |
| 19–24 | $1^-$ | 2·08 | 2·230 | | |
| 19–35 | $1^-$ | 2·08 | 3·860 | | |

[A] Relative to the $^{12}$C ground state.

and for magnetic multipole transitions

$$\sum_{M_i M_f} |\mathscr{M}|^2_{ML} = 8\pi \sum_{L'=L\pm1} I^*_{LL'}(T)\, I_{LL'}(T), \tag{21}$$

$$\sum_{M_i M_f} |\hat{k}_\gamma . \mathscr{M}|^2_{ML} = 8\pi \,\mathrm{Re}\Bigg[ \sum_{L'=L\pm1} \sum_{L''=L\pm1} I^*_{LL'}(T)\, I_{LL''}(T) \times \Bigg( \tfrac{1}{3}\delta_{L'L''} + (-)^L (\tfrac{3}{2})^{\frac{1}{2}} \langle L'L''00|20\rangle \times \{(2L'+1)(2L''+1)\}^{\frac{1}{2}} \begin{Bmatrix} L' & L'' & 2 \\ 1 & 1 & L \end{Bmatrix} \{(\hat{k}_\gamma . \hat{T})^2 - \tfrac{1}{3}\} \Bigg) \Bigg], \tag{22}$$

where

$$\hat{k}_\gamma . \hat{T} = (k_\gamma - \alpha p_\pi \cos\theta)/T . \tag{23}$$

The plane wave limit of the ADWA in which $(\alpha, \beta)$ is $(1, 0)$ clearly gives the generalized Helm model results so that our scheme is a most obvious way of ascertaining the role of distortion of the pion wavefunction in both real and virtual photoproduction cross sections.

## 3. ADWA for Low Energy Pions

In order to ascertain the optimum values for the parameters of our analytic functions we fit pion elastic scattering data over the range of energies required. This is accomplished by using the Kisslinger form of the optical potential, namely

$$U(r) = -\{A(\hbar c)^2/2E\}\{b_0\, k_i^2\, \rho(r) - b_1 \nabla . \rho(r) \nabla\}, \tag{24}$$

in the integral form of the scattering amplitude

$$f(\theta) = -\frac{\mu}{2\pi\hbar^2}\int \exp(-\mathrm{i}\boldsymbol{k}_\mathrm{f}.\boldsymbol{r})\, U(r)\,\psi^{(\pm)}_{k_\mathrm{i}}(r)\,\mathrm{d}r. \tag{25}$$

In our ADWA scheme and in the small $\beta$ limit this results in (Di Marzio and Amos 1983, 1985*a*, 1985*b*; Amos and Di Marzio 1984)

$$f^{\mathrm{ADWA}}(\theta) = (A\mu N/E)\{(b_0\, k_\mathrm{i}^2 + b_1|\boldsymbol{K}_\mathrm{i}|^2)I_1 + 2b_1\, K_\mathrm{i}\cos\epsilon\, I_2\}, \tag{26}$$

where

$$\boldsymbol{K}_\mathrm{i} = (\alpha+\mathrm{i}\beta)\boldsymbol{k}_\mathrm{i}, \tag{27}$$

$$I_1 = \int_0^\infty \mathrm{j}_0(T'r)\,\rho(r)r^2\,\mathrm{d}r, \tag{28}$$

$$I_2 = \int_0^\infty \mathrm{j}_1(T'r)\{\rho_0\,\eta\,\exp(-r^2/a_\rho^2) - \rho(r)/a_\rho^2\}\,r^3\,\mathrm{d}r, \tag{29}$$

with

$$\epsilon = \tfrac{1}{2}(\pi-\theta) - \arcsin[(\alpha-1)k_\mathrm{i}\,\sin\{\tfrac{1}{2}(\pi-\theta)\}/T']. \tag{30}$$

Here we have

$$\boldsymbol{T}' = \alpha\boldsymbol{k}_\mathrm{i} - \boldsymbol{k}_\mathrm{f} \tag{31}$$

and therefore

$$T' = [\{(\alpha-1)k_\mathrm{i}\}^2 + 2q(\alpha-1)k_\mathrm{i}\cos\tfrac{1}{2}(\pi-\theta) + q^2]^{\frac{1}{2}}, \tag{32}$$

and

$$\rho(r) = \rho_0(1+\eta r^2)\exp(-r^2/a_\rho^2) \tag{33}$$

is the nuclear density distribution with

$$\rho_0 = 4/A(\pi^{\frac{1}{2}}a_\rho)^3, \qquad \eta = (A-4)/6a_\rho^2. \tag{34, 35}$$

The values of $a_\rho$ chosen are those that most closely match the nuclear density profiles others (Blecher *et al.* 1979; Preedom *et al.* 1981; Obenshain *et al.* 1983) have used in determining the ideal optical potential parameters ($b_0$, $b_1$) which best reproduce their low energy experimental data. These are displayed in Table 2.

At low pion incident energies Coulomb effects are important; they are included through the amplitude (Amos and Di Marzio 1985)

$$f^{\mathrm{Coul}}(\theta) = \zeta^2\sinh(\pi\zeta)\{\Gamma(\mathrm{i}\zeta)\}^2\exp\{-2\mathrm{i}\zeta\ln(\sin\tfrac{1}{2}\theta)\}/2\pi k\sin^2\tfrac{1}{2}\theta, \tag{36}$$

where

$$\zeta = Z_1 Z_2 e^2/\hbar v. \tag{37}$$

Hence the differential cross sections for elastic scattering may be evaluated from

$$\mathrm{d}\sigma/\mathrm{d}\Omega\ (\mathrm{mb\,sr^{-1}}) = 10|f^{\mathrm{ADWA}}(\theta) + f^{\mathrm{Coul}}(\theta)|^2, \tag{38}$$

enabling the derivation of the proper ADWA forms for the pion continuum wavefunctions to be employed in the non-elastic reactions.

**Table 2. Kisslinger potential and ADWA parameters for the elastic scattering of low energy positive pions at various incident energies**

| Nucleus | $a_\rho$ (fm) | $E_\pi$ (MeV) | $b_0$ (fm$^3$) | $b_1$ (fm$^3$) | $\alpha$ | $\beta$ |
|---|---|---|---|---|---|---|
| $^{12}$C | 1·6 | 20 | −4·38−i1·48 | 5·48−i0·11 | 1·05 | −0·1 |
| | | 30 | −4·13−i0·04 | 6·26+i1·22 | 0·8 | −0·065 |
| | | 40 | −3·33+i0·19 | 6·17+i1·16 | 0·5 | 0 |
| | | 50 | −3·26+i0·46 | 6·60+i0·69 | 0·2 | 0·065 |
| $^{16}$O | 1·7 | 20 | −4·53+i2·27 | 5·25−i1·36 | 1·05 | 0·115 |
| | | 30 | −4·14−i0·13 | 6·51+i1·55 | 0·7 | 0·02 |
| | | 40 | −3·60−i0·16 | 6·45+i1·41 | 0·55 | 0 |
| $^{40}$Ca | 2·3 | 20 | −4·60+i3·11 | 4·93−i2·31 | 0·9 | 0·22 |
| | | 30 | −4·01+i0·08 | 6·00+i0·58 | 0·75 | 0·05 |
| | | 40 | −3·04−i0·04 | 5·79+i1·14 | 0·65 | 0·035 |

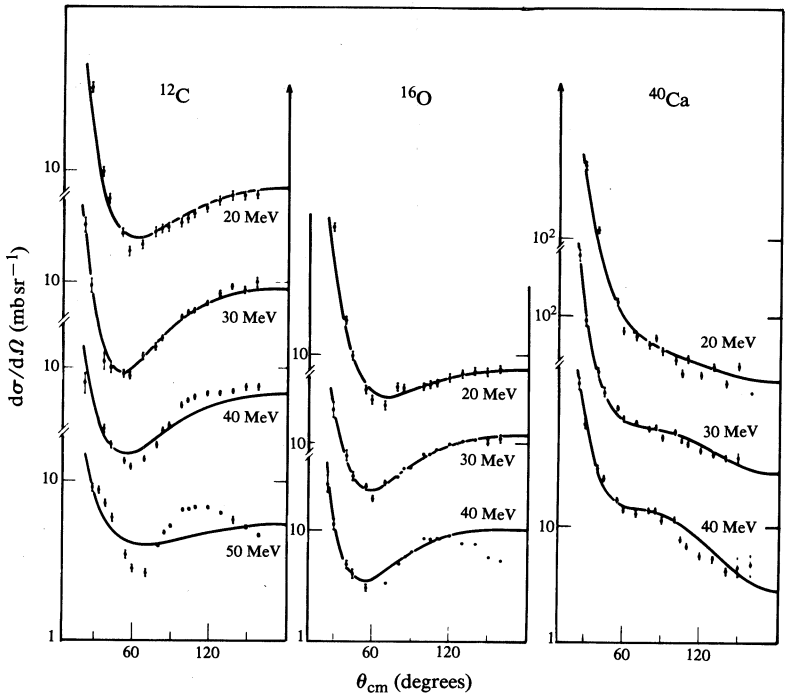


**Fig. 1.** ADWA predictions compared with the elastic scattering data of $\pi^+$ from $^{12}$C, $^{16}$O and $^{40}$Ca at the kinetic energies indicated.

Specifically, we have used the ADWA scheme to obtain the best fits possible to the $\pi^+$ elastic scattering differential cross sections from $^{12}$C, $^{16}$O and $^{40}$Ca at incident energies of 20, 30 and 40 MeV, and for $^{12}$C at 50 MeV as well. The results of these calculations are depicted in Fig. 1 for the smoothly varying (with energy) parameter values listed in Table 2. The 20, 30 and 40 MeV data are fitted quite well by our ADWA calculation results, but the 50 MeV (and to a lesser extent the 40 MeV) data comparison is rather poor, signifying a sensitivity to s- and p-wave amplitude

interference that is due to the onset of important contributions from short range correlations (Lorentz–Lorenz effect), Pauli blocking, nuclear medium corrections and so on. In fact, at energies less than about 40 MeV our predictions are very similar to those made using full distortion, thus justifying the ADWA and indicating that low energy pions possess significant mean free paths as the result of the transparent nature of nuclei to pions in this energy region. This also explains, in part, why the generalized Helm model has been reasonably successful in describing nuclear reactions of this kind.

Moreover, since in this study the emergent pion energies for both photopion and electropion production are typically between 30 and 40 MeV, then the validity of our ADWA in analyses of these nuclear reactions is clearly substantiated and gives at least a good indication of the appropriate values for the ADWA parameters.

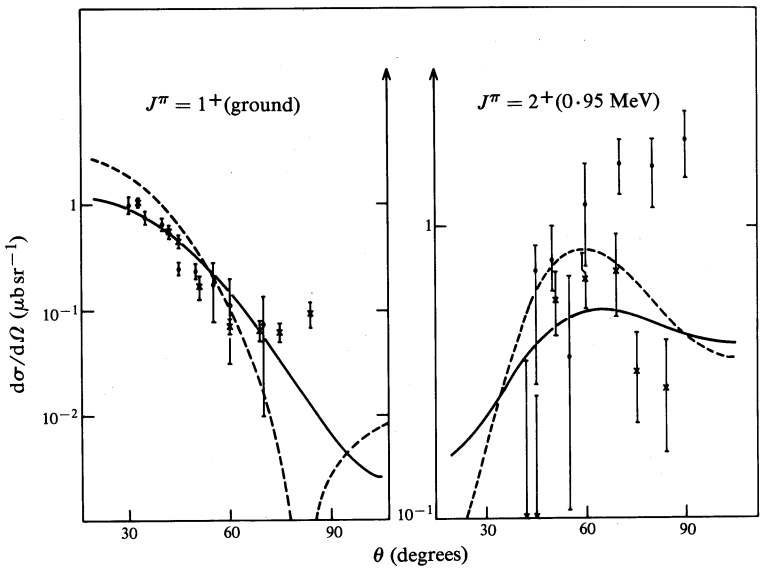


**Fig. 2.** Results from the ADWA (solid curves) and plane wave (dashed curves) Helm model calculations compared with the photopion production data for the reaction $^{12}C(\gamma,\pi^+)^{12}B(J^\pi)$ ($E_\gamma$ = 194 MeV). The data of Shoda *et al.* (1980) are represented by the solid circles and those of Schmitt *et al.* (1983) by the crosses.

## 4. ADWA and Pion Production

### *(a) Helm Model Studies*

By using the results of the ADWA analyses of elastic scattering from $^{12}C$, one would anticipate the $(\alpha,\beta)$ values required in the $^{12}C(\gamma,\pi^+)^{12}B$ reaction to be (0·65, −0·03), although some variation is possible as the residual nucleus is $^{12}B$ rather than $^{12}C$. In particular, and unlike $\alpha$, the parameter $\beta$ is quite sensitive to the type of nucleus. In fact, the best simultaneous fit to the photopion data leading to the ground and first excited states in $^{12}B$ is obtained using the values (0·65, 0·0007). The results of using the ADWA are compared with the (plane wave) Helm model calculations and with the data in Fig. 2. The ADWA results were obtained using

the same transition density matrices as used in the Helm model calculations, whereby comparison of the two calculated results gives a measure only of the distortion effects. However, in so far as the density matrices are determined from the relevant electron scattering form factors, comparison with the data clearly reveals that distortion effects are essential in data analyses. Furthermore, the more recent $2^+$ data (Schmitt *et al.* 1983) are clearly favoured over the older versions—and more so when distortion effects are considered.

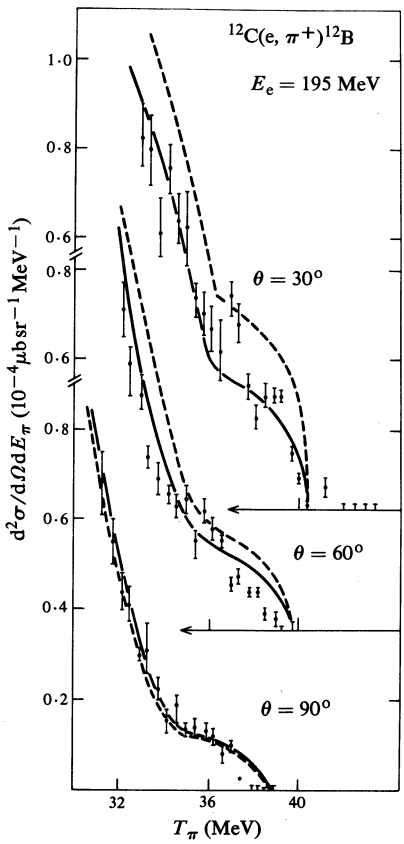


**Fig. 3.** Results of the ADWA (solid curves) and plane wave (dashed curves) Helm model calculations of the electropion production cross sections at the scattering angles indicated.

The electropion production calculation results are compared with data (Shoda *et al.* 1980) in Fig. 3, from which it is evident that the ADWA version of the Helm model again gives results that are distinguishably different from the usual (plane wave) version and that are in very good agreement with the data. The results of these analyses complement those of the photopion reactions in that the electropion cross sections are functions of the outgoing pion kinetic energies. Clearly the smooth ADWA variation of distortion parameters that we obtained from our analyses of (low energy) pion elastic scattering is appropriate. Specifically, the ADWA predictions reproduce the data at all available angles whilst the Helm model fails at small scattering angles. This observation can be anticipated since, when $\alpha < 1$, we get $q < T$ for small $\theta$, which results in smaller values for the arguments of the spherical Bessel functions in the transition form factors. Hence, the usual Helm model has larger contributions from these form factors for small $\theta$. For large scattering angles

however, notably for $\theta = 90°$, the Helm and ADWA results are almost identical since in this case $q \sim T$.

*(b) Microscopic Structure Model Studies*

The many body nuclear matrix elements of equation (10) involve a sum of one body operators and as such they may be cast as the sum of one body expectation values weighted by the spectroscopic amplitudes

$$S_{j_1 j_2 J} = \langle {}^{12}\mathrm{B};\ J^\pi \| [a^{(+)\dagger}_{j_2} \times a^{(-)}_{j_1}]^J \| {}^{12}\mathrm{C};\ \text{ground} \rangle, \tag{39}$$

in which $a^{(-)}_{j_1}$ annihilates a proton in orbit $j_1$ and $a^{(+)\dagger}_{j_2}$ creates a neutron in orbit $j_2$. Given a nuclear structure model from which these numbers may be estimated, and a model for the spatial variation of the single particle orbits (an harmonic oscillator with $\hbar\omega = 14{\cdot}9$ MeV was used), then the transition densities in equation (16) are readily obtained.

We suppose that the $^{12}$B states ($J^\pi$; $1^+$ and $2^+$) are the simple isobaric analogues of the $1^+$ and $2^+$ isovector states in $^{12}$C, so that the transition densities for real and virtual photopion production can be related to the transition densities for inelastic scattering to the relevant states in $^{12}$C; this premise underlies the Helm model studies reported previously. Thus, we consider

$$|{}^{12}\mathrm{B};\ J^\pi\rangle = N \sum_{jm} a^{(+)\dagger}_{jm}\, a^{(-)}_{jm} |{}^{12}\mathrm{C};\ J^\pi\rangle, \tag{40}$$

for which the normalization is

$$N^{-2} \equiv \sum_{jmj'm'} \langle {}^{12}\mathrm{C};\ J^\pi |\, a^{(-)\dagger}_{j'm'}\, a^{(+)}_{j'm'}\, a^{(+)\dagger}_{jm}\, a^{(-)}_{jm} |{}^{12}\mathrm{C};\ J^\pi\rangle \tag{41}$$

$$\equiv \sum_j (2j+1)\sigma^{(J^\pi)}_j(\mathrm{p})\{1-(2j+1)\sigma^{(J^\pi)}_j(\mathrm{n})\}, \tag{42}$$

in which $\sigma^{(J^\pi)}_j(x)$ is the fractional occupancy of orbit $j$ in the state $|{}^{12}\mathrm{C};\ J^\pi\rangle$ for a particle of type $x$. Thus, we further consider

$$S_{j_1 j_2 J} = \langle {}^{12}\mathrm{B};\ J^\pi \| [a^{(+)\dagger}_{j_2} \times a^{(-)}_{j_1}]^J \| {}^{12}\mathrm{C};\ \text{ground} \rangle \tag{43}$$

which, when multiparticle–multihole contributions are ignored, becomes

$$S_{j_1 j_2 J} = N \sum_\nu (-)^{\frac{1}{2}+\nu} \langle {}^{12}\mathrm{C};\ J^\pi \| [a^{(\nu)\dagger}_2 \times a^{(\nu)}_{j_1}]^J \| {}^{12}\mathrm{C};\ \text{ground} \rangle, \tag{44}$$

from which

$$\rho_{j_1 j_2}({}^{12}\mathrm{B};\ J^\pi) = N \sum_\nu (-)^{\frac{1}{2}+\nu} \rho_{j_1 j_2}({}^{12}\mathrm{C};\ J^\pi\ T=1) \tag{45}$$

is the specific 'simple' model relationship in terms of the $^{12}$C inelastic scattering transition densities. Under the same assumptions, the normalization may be readily ascertained by the specification

$$\sigma^{(J^\pi)}_j(\nu) = S^{(\nu)}_{j_1 j_2 J}({}^{12}\mathrm{C};\ J^\pi)/(2j_2+1), \tag{46}$$

**Table 3. Proton spectroscopic amplitudes for the excitation of the isovector $1^+$ (15·11 MeV) and $2^+$ (16·11 MeV) states in $^{12}C$**

| $j_1$ | $j_2$ | $S^{SM}_{j_1j_2}(1^+)$ | $S^{PHM}_{j_1j_2}(1^+)$ | $S^{SM}_{j_1j_2}(2^+)$ | $j_1$ | $j_2$ | $S^{SM}_{j_1j_2}(1^+)$ | $S^{PHM}_{j_1j_2}(1^+)$ | $S^{SM}_{j_1j_2}(2^+)$ |
|---|---|---|---|---|---|---|---|---|---|
| $0p_1$ | $0p_1$ | 0·071 | −0·128 | | $0s_1$ | $0d_3$ | | 0·047 | |
| $0p_3$ | $0p_1$ | 0·845 | 0·578 | 1·074 | $1s_1$ | $0d_3$ | | 0·006 | |
| $0p_1$ | $0p_3$ | 0·416 | 0·490 | −0·180 | $0p_1$ | $1p_1$ | | 0·020 | |
| $0p_3$ | $0p_3$ | 0·093 | 0·167 | 0·096 | $0p_3$ | $1p_1$ | | 0·005 | |
| $1p_1$ | $0p_1$ | | 0·014 | | $0p_1$ | $1p_3$ | | −0·025 | |
| $1p_3$ | $0p_1$ | | 0·084 | | $0p_3$ | $1p_3$ | | −0·031 | |
| $1p_1$ | $0p_3$ | | 0·055 | | $0p_3$ | $0f_5$ | | 0·027 | |
| $1p_3$ | $0p_3$ | | 0·032 | | $0p_3$ | $0f_5$ | | 0·004 | |
| $0f_5$ | $0p_3$ | | −0·011 | | $1f_7$ | $0f_5$ | | 0·011 | |
| $0s_1$ | $1s_1$ | | −0·016 | | | $N$ | 0·6557 | 0·7135 | 0·6765 |

so that for each $^{12}C$ $J^\pi$ state set of spectroscopic amplitudes

$$N = \left( \sum_{j_1 j_2} S^{(-)}_{j_1 j_2} (1 - S^{(+)}_{j_1 j_2}) \right)^{-\frac{1}{2}} . \tag{47}$$

The values of the $1^+$(15·11 MeV) and $2^+$(16·11 MeV) isovector excitation spectroscopic amplitudes (in $^{12}C$) previously used to analyse inelastic scattering data (Amos *et al.* 1981) (of electrons, protons and, more recently, pions) are given in Table 3, as are the normalization values $N$ obtained by their use in equation (47). The columns identified by the superscript SM contain the results using the Cohen and Kurath (CK) p-shell model description, whilst the label PHM signifies the particle–hole model results (Amos *et al.* 1981). The PHM values are not given for the $2^+$ state excitation as they are not a realistic prescription, having a marked reduction in the 0p shell transition strength as opposed to the (more realistic) CK values. In particular, the largest CK spectroscopic amplitude arises for the $0p_{3/2} \rightarrow 0p_{1/2}$ transition ($S^{SM}_{j_1j_2} = 1·074$) for which the corresponding PHM value is only 0·393. Conversely, the strongest transition ($S^{PHM}_{j_1j_2} = 0·725$) in the PHM occurs for $0p_{3/2} \rightarrow 0p_{3/2}$, whereas the CK value (0·096) for this transition is almost eight times smaller. Furthermore, calculations performed with the PHM spectroscopy reveal very strong cancellations for contributions amongst the 0p shell (Amos *et al.* 1981).

Use of these microscopic transition densities in analyses of the photopion data yield the results that are compared with the data in Fig. 4. The ADWA calculation of the ground state transition gives the general trend of the data but clearly does not have the appropriate momentum transfer variation, being a factor of 2 too small at forward angles and too large at larger scattering angles. Since this spectroscopy predicts a $B$(M1) value of $2·77\mu_N^2$, which is in excellent agreement with the experimental value of $2·78\mu_N^2$, and calculations using this structure compare quite favourably with proton scattering data (at least for momentum transfers less than about 1·5 fm$^{-1}$), this result already suggests that our modelling of the structure of states in $^{12}B$ from the corresponding states in $^{12}C$ may be too naive.

The PHM structure, on the other hand, is expected to be less reliable than the SM since the effective 0p shell splitting is too small, resulting in an underestimation of recoupling strengths within the 0p shell. As a consequence the PHM predictions for the isovector transverse form factor are down by a factor of 3·2 (Amos *et al.* 1981).

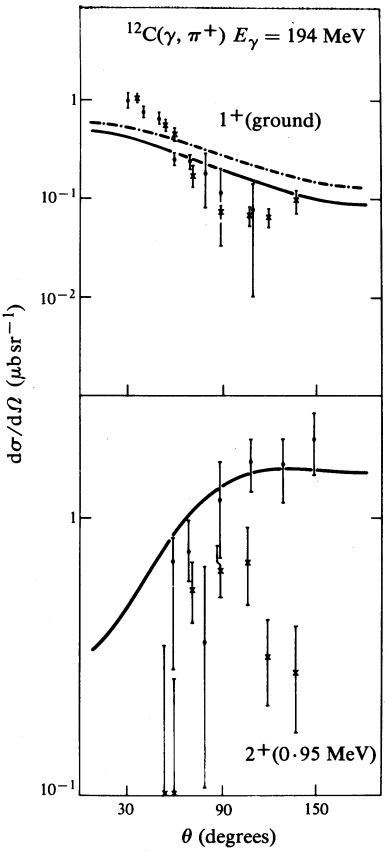


**Fig. 4.** Microscopic structure model results using the ADWA for the photopion reactions. The solid curves depict the results obtained using the SM transition densities, whilst the dashed curve gives those of the PHM values.

The PHM cross-section predictions in Fig. 4 have thus been scaled up by this factor and are then seen to be similar in shape (although some 25–50% larger in magnitude) to the SM results.

With respect to the $2^+$ state, the SM spectroscopy overestimates the electron scattering form factors by a factor of 2 and so our photopion calculation results have been scaled accordingly. The predictions then fit the data of Shoda *et al.* (1980), but this may be simply fortuitous as the naiveté of our model structure coupled with the onset of competing processes could quite conceivably influence the results. In any case the Helm model does not suffer from any of these shortcomings and, as such, indicates that the SM results are approximately a factor of 2 larger in magnitude than those generated using a 'correct' model of nuclear structure.

## 5. Conclusions

An analytic distorted wave approximation has been developed and applied to analyse photopion and electropion production differential cross sections from $^{12}C$ and near threshold. The ADWA form of the Helm model produces fits to the existing photopion data (with $E_\gamma \sim 194$ MeV), leading to the ground and first excited states in $^{12}B$, which are superior to the usual generalized Helm model predictions. In particular, the results for the isovector $2^+$ state in $^{12}B$ distinctively underestimate the data of Shoda *et al.* (1980) but are in good agreement with those of Schmitt *et al.* (1983), indicating that the latter are the more reliable of the two. Moreover,

the improvement in both shape and magnitude over the usual Helm model clearly demonstrates the importance of pion distortion. This importance was confirmed as the inclusion of distortion also led to a marked improvement in the predictions for electropion production cross sections, especially at small scattering angles. At larger scattering angles both the Helm model and its ADWA analogue give excellent fits to this data.

Analyses of low energy positive pion elastic scattering, but more importantly, a close matching of the complete optical model elastic scattering differential cross sections demonstrate that the ADWA prescription for distortion is reasonable for 20, 30 and 40 MeV positive pions incident upon $^{12}C$, $^{16}O$ and $^{40}Ca$, as well as determining a base set of parameters $(\alpha, \beta)$ (smoothly varying in energy). Some adjustment to the values of $\beta$ is required to give optimal results when the ADWA is used to analyse the pion production data; this is due, we believe, to the fact that the pions emerge from $^{12}B$ and not $^{12}C$. The same values, however, were used to analyse the data from both the $1^+$ and $2^+$ states in $^{12}B$.

Finally, we considered two models of (microscopic) nuclear structure, replacing the Helm model transition densities previously used by a simple isobaric analogue prescription for the $^{12}B$ state in relation to the 15·11 and 16·11 MeV states in $^{12}C$. The Cohen and Kurath 0p shell model was used to ascertain transition densities for both transitions, and a large basis model of particle–hole excitations upon a Hartree–Fock minimal energy determinant was used for the ground state transition as well. Their use in analyses of data from photopion production leading to the $^{12}B$ ground state reveals that both the SM and PHM calculations have a similar shape but underestimate the forward scattering by a factor of 2, whereas for the first excited state in $^{12}B$ the predictions possess the correct shape but overestimate the data by the same factor. We conclude that our nuclear structure model is as yet too simple to properly account for all the main features of the data.

## Acknowledgments

This research was supported by a grant from the Australian Research Grants Scheme and one of us (F.DiM.) gratefully acknowledges the financial support of a Commonwealth Postgraduate Research Award.

## References

Amos, K., and Di Marzio, F. (1984). *Phys. Rev.* C **29**, 1914.
Amos, K., and Di Marzio, F. (1985). *Z. Phys.* A **322**, 137.
Amos, K., Morrison, I., Smith, R., and Schmid, K. W. (1981). *Aust. J. Phys.* **34**, 493.
Blecher, M., *et al.* (1979). *Phys. Rev.* C **20**, 1884.
Cannata, F., *et al.* (1974). *Can. J. Phys.* **52**, 1405.
Dalitz, R. H., and Yennie, D. R. (1957). *Phys. Rev.* **105**, 1598.
Di Marzio, F., and Amos, K. (1983). *Aust. J. Phys.* **36**, 135.
Di Marzio, F., and Amos, K. (1985*a*). *Phys. Rev.* C **31**, 561.
Di Marzio, F., and Amos, K. (1985*b*). *Phys. Lett.* B **153**, 13.
Epstein, G. N., Singham, M. K., and Tabakin, F. (1978). *Phys. Rev.* C **17**, 702.
Furui, S. (1978). *Nucl. Phys.* A **300**, 385; A **312**, 311.
Haxton, W. (1980). *Phys. Lett.* B **92**, 37.
Nagl, A., and Überall, H. (1976). *Phys. Lett.* B **63**, 291.
Obenshain, F. E., *et al.* (1983). *Phys. Rev.* C **27**, 2753.
Preedom, B. M., *et al.* (1981). *Phys. Rev.* C **23**, 1134.

Schmitt, Ch., Röhrich, K., Maurer, K., Ottermann, C., and Walther, V. (1983). *Nucl. Phys.* A **395**, 435.
Shoda, K., Ohashi, H., and Nakahara, K. (1980). *Nucl. Phys.* A **350**, 377.
Singham, M. K., Epstein, G. N., and Tabakin, F. (1979). *Phys. Rev. Lett.* **43**, 1476.
Singham, M. K., and Tabakin, F. (1981). *Ann. Phys. (New York)* **135**, 71.
Überall, H. (1971). 'Electron Scattering from Complex Nuclei' (Academic: New York).

Manuscript received 6 September, accepted 28 November 1985